Ferroelectrics, 1993, Vol. 139, pp. 25–49
Reprints available directly from the publisher
Photocopying permitted by license only

ELECTROMECHANICAL NONLINEARITY OF FERROELECTRIC CERAMICS AND RELATED NON-180° DOMAIN WALL MOTIONS

SHAOPING LI, WENWU CAO, R. E. NEWNHAM and L. E. CROSS
Materials Research Laboratory, The Pennsylvania State University, University Park, PA 16802 USA

(Received June 13, 1992; in final form August 26, 1992)

Using an optical interferometer and other experimental techniques, the mechanical and dielectric response of lead zirconate titanate $Pb(Zr_xTi_{1-x})O_3$ ceramics to an a.c. electric field have been investigated directly. The experimental results demonstrate the importance of the domain wall motion in generating the electromechanical nonlinearities in ferroelectric ceramics. It has been verified that the couplings between the acoustic vibrations and the movement of domain walls is an important factor in terms of extrinsic properties of ferroelectric polycrystalline materials. A phenomenological theory has been extended to describe the extrinsic contributions to the piezoelectric, elastic and dielectric properties. These effects can be attributed to both the linear and nonlinear vibrations of non-180° domain walls in ferroelectric ceramics. The proposed theory shows qualitative agreement with the experimental results.

Keywords: ferroelectric ceramic, PZT, nonlinearity, domain walls, piezoelectricity

I. INTRODUCTION

Electromechanical nonlinearity in ferroelectric polycrystalline materials is an important problem in modern ultrasonic engineering. Ferroelectric ceramics are widely used as transducers, resonators, actuators, motors, and capacitors which represent a very large segment of the electroceramics market. One of the limitations of ferroelectric transducers for practical use are the nonlinear effects which occur at high drive level,[1–6] because ferroelectric ceramics are the strongest known nonlinear piezoelectric materials.[7] Moreover, techniques for fabricating ferroelectric thin films have made great progress during recent years leading to the possibility of utilizing nonlinear phenomena of ferroelectric polycrystalline thin film devices in conjunction with integrated circuits. Significant nonlinear phenomena in thin films can be observed under voltages of less than a volt. In practical applications, the nonlinearity of ferroelectric polycrystalline materials directly influences the performance of microwave acoustic devices such as convolvers and correlators.[7–9] The so-called "smart ceramic systems"[10] incorporating sensors and actuators also need to exploit the nonlinear properties of ferroelectric ceramics. In short, on certain occasions, one wants to avoid the nonlinearities, while on other occasions one wants to benefit from them. Therefore, from a technological point of view, it is important to study the nonlinear electromechanical properties in ferroelectric ceramics so as to optimize the choice of piezoceramics most suitable for transducers, actuators, resonators, ultrasonic motors and other acoustic devices, as well as to

develop new types of nonlinear electronic devices such as frequency mixers and doublers, and piezoelectric thin film devices.

The piezoelectric effects in ferroelectric ceramics are caused by two mechanisms: (1) the intrinsic piezoelectric effect[11-12] connected with the deformation of each unit cell of the ferroelectric material by an electric field and (2) the extrinsic piezoelectric effect[13-15] that, for example in lead zirconate titanate (PZT) system, refers to the motion of non-180° domain walls and the movement of the interphase phase boundary between the tetragonal and rhombohedral phase regions.[16] It is believed that the piezoelectric effect in polycrystalline ferroelectrics is caused not only by the ionic displacement in connection with the change of the polarization magnitude, but also by the movements of domain walls and interphase boundaries. Studies on materials such as $BaTiO_3$ and PZT[17] have shown that as much as 60%–70% of the piezoelectric moduli values may originate from the extrinsic contributions. In fact, the performance of many transducers, actuators and capacitors are based on the control of domain structures under applied electric field. Microstructure investigations[18-20] showed that the poled ferroelectric ceramics contain a large number of non-180° domain boundaries which strongly affect their electromechanical behavior.[21-27] In general, these domain structures give rise to complex linear and nonlinear behavior which is very sensitive to the quality of the sample and its defect concentration, as well as the external boundary conditions.

Even though the investigation of the electromechanical nonlinearity in ferroelectrics has been carried on for the last three decades, most of the studies[28-30] are based on thermodynamic theory only, without considering the dynamics of domain walls. Very little work[31,32] has been done to describe the behavior of electromechanical nonlinearity in terms of domain wall motion, even though the domain wall motion plays a dominant role over a wide range of external field levels, and also the frequency response of domain wall motions spans a range from almost zero hertz to the microwave regime. Moreover, a number of ambiguities still remain in this area due to the lack of sufficient information about the relationship between electromechanical coefficients and the motions of non-180° domain walls and the movement of interphase boundaries.

Here, it should be mentioned that one of the challenges facing materials scientists is to develop a scientific foundation for the understanding and the rational design of sophisticated material systems with novel microstructures as well as multiple functional characteristics. At present, the major shift in ferroelectric research and development is underway from single-crystal devices to fully integrated polycrystalline thin film devices in which the ferroelectric elements are an integral part of the silicon or GaAs integrated circuit, or very elegant micro-transducers with multiple functions for various applications. The key issue for this development is from general qualitative investigation of physical properties of polycrystalline materials towards more quantitative examination of the relationship between the microstructures and macroscopic properties. Basically, it has been known that one of the simplest types of composite with piezoelectric constituents is a single phase polycrystalline aggregate, with grains made of the same piezoelectric substance but with mismatched orientations of the crystallographic axes at the grain boundaries. Since the micro-piezoelectricity combining micromechanics and microelectronics is of great significance in microferroelectricity, the quantitative study of the rela-

tionship between the microstructure and related properties in polycrystalline materials is the basis for further development in microferroelectricity.

It is the objective of this work to evaluate the linear and nonlinear elastic, dielectric, and piezoelectric coefficients arising from the domain wall motions, and to form a tentative model based on the observed linear and nonlinear effects in an attempt to gain some physical insight into the relationship between domain wall motions and nonlinear electromechanical properties in ferroelectric ceramics. This paper is structured as follows: in sections II and III, we present a general description of the electromechanical properties arising from the non-180° domain wall motions in the ferroelectric ceramic. Through considering the macroscopic nonlocal motion of domain walls in the presence of external fields, we obtain expressions for a number of experimentally accessible quantities. In section IV, we show some experimental results which characterize the dynamic electromechanical response of the PZT ferroelectric ceramics. Some of the experimental results strongly support our approach to the problem.

II. THEORETICAL

2.1. Domain and Interphase Structures

In a $Pb(Zr_xTi_{1-x})O_3$ system with composition near the morphotrophic phase boundary, the tetragonal and rhombohedral phases coexist. Therefore, besides the 180° domain wall, there are 71°, 110° and 90° domain walls. Also interphase boundaries between the two phases exist. Here, we do not discuss the case for 180° domain walls. The 180° domain wall motion does not significantly affect the piezoelectric and electromechanical properties because the spontaneous deformations of the antiparallel domains are the same.[61,62] In order to investigate systematically the relationship between linear piezoelectric effect and the non-180° domain wall motions in ferroelectric ceramics, Arlt *et al.*[13,14] first presented a phenomenological model for the vibrating 90°-domain wall under electric field and mechanical stress to describe the linear piezoelectric behavior of ferroelectric ceramics. We have generalized this model to describe the nonlinear effects resulting from the vibrating 90°-domain walls.[33]

Here, we will try to model non-180° domain wall motions for the cases of rhombohedral phase and interphase conversion between the tetragonal and rhombohedral regions, respectively. As we know, the symmetry of the ferroelectric phase is fully determined by the symmetry of the parent phase. The spontaneous polarization has equal probability to lie in all the equivalent directions prescribed by the prototypic form from which the ferroelectric phase is derived. From phenomenological theory,[12] we can find eight energetically equivalent variants in the rhombohedral ferroelectric stable states of PZT system as following:

$$\begin{aligned} &\text{I. } (P_1, P_2, P_3), \quad \text{II. } (P_1, P_2, -P_3), \quad \text{III. } (-P_1, P_2, P_3), \\ &\text{IV. } (P_1, -P_2, P_3), \quad \text{V. } (-P_1, P_2, -P_3), \quad \text{VI. } (P_1, -P_2, -P_3), \\ &\text{VII. } (-P_1, -P_2, P_3), \quad \text{VIII. } (-P_1, -P_2, -P_3) \end{aligned} \tag{1}$$

where $P_i (i = 1, 2, 3)$ are the components of the spontaneous polarization P_0 in

Cartesian coordinates, $P_1^2 = P_2^2 = P_3^2 = P_0^2/3$. Accordingly, the spontaneous strain under zero stress conditions can be written as:

$$S_{11} = S_{22} = S_{33} = (Q_{11} + 2Q_{12})P_0^2/3$$
$$S_{12} = Q_{44}P_1P_2, \quad S_{23} = Q_{44}P_2P_3, \quad S_{13} = Q_{44}P_1P_3 \tag{2}$$

where, Q_{ij} are the electrostrictive coefficients. Obviously, the normal components of s_{ii} are the same for all of the orientation states, and the shear components of the spontaneous strain tensor in the corresponding Equation (1) have the following forms:

$$\text{I(VIII)}.\ S_{12} = S_{23} = S_{31} = \frac{Q_{44}}{3}P_0^2; \quad \text{II(VII)}.\ S_{12} = -S_{23} = -S_{31} = \frac{Q_{44}}{3}P_0^2;$$
$$\text{III(VI)}.\ S_{12} = -S_{23} = S_{31} = \frac{-Q_{44}}{3}P_0^2;$$
$$\text{IV(V)}.\ S_{12} = S_{23} = -S_{31} = \frac{-Q_{44}}{3}P_0^2 \tag{3}$$

These eight low temperature variants will form 180°, 71° and 110° twin structures. For instance, the polarization vectors in a twin structure between states (I) and (VII) form a angle θ,

$$\theta = \cos^{-1}(\vec{n}_{111}\cdot\vec{n}_{\bar{1}\bar{1}1}) = \cos^{-1}\left(\frac{-1}{3}\right) = 110°$$

where $\vec{n}_{111}$ and $\vec{n}_{\bar{1}\bar{1}1}$ are unit vectors in [111] and $[\bar{1}\bar{1}1]$, respectively. The twin boundary is then called 110° domain wall. We choose primed and unprimed coordinate systems for a basic piezoelectric element as shown in Figure 1, which contains a single 110° domain wall and separates the polarization states (I) and (VII). In the primed system, domain wall is located in $z' = 0$ plane.[24] A displacement Δl of the domain wall gives rise to a change in the electric dipole moment δP_i in volume ΔlA,[34,35]

$$\vec{\delta P'} = \frac{2}{\sqrt{3}}\Delta l A P_0 \begin{bmatrix}1\\1\\0\end{bmatrix} \tag{4}$$

Δl is the displacement of the domain wall and A is the area of the vibrating domain wall per unit volume. This movement of domain walls also induce a change in the elastic dipole moment, which in the primed coordinate can be written as

$$\delta\tilde{U}' = \Delta l A S_0 \begin{bmatrix}0 & 0 & 1\\0 & 0 & 1\\1 & 1 & 0\end{bmatrix} \tag{5}$$

where,

$$S_0 = \frac{2Q_{44}}{3}P_0^2$$

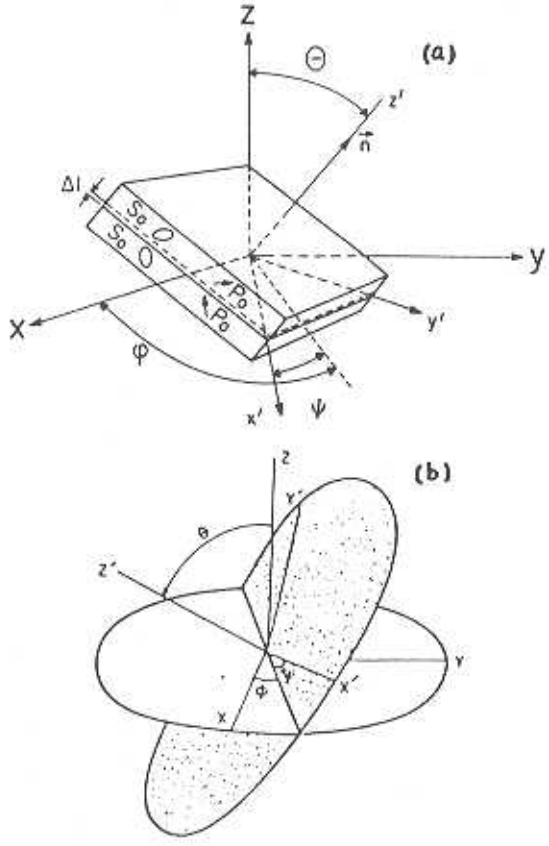

FIGURE 1 (a) A basic element of a twin structure in a rhombohedral ferroelectric ceramic. (b) The unprimed and primed coordinate systems. The relative orientation is characterized by the Eulerian angles (ϕ, ψ, θ).

where, P_0 and S_0 are the spontaneous polarization and strain, respectively, in the rhombohedral phase. Finally, in (x, y, z) coordinate system, the changes of induced electric and elastic dipoles can be obtained through a coordinate transformation:

$$\delta P_i = \Delta l A P_0 f_i(\Theta, \Phi, \Psi) \tag{6}$$

and,

$$\delta U_{ij} = \Delta l A S_0 F_{ij}(\Theta, \Phi, \Psi) \tag{7}$$

where

$f_1 = [\cos\Phi(\cos\Psi - \sin\Psi) - \cos\Theta \sin\Phi(\sin\Psi + \cos\Psi)]$, $f_2 = [\sin\Phi(\cos\Psi - \sin\Psi) + \cos\Theta \cos\Phi(\sin\Psi + \cos\Psi)]$, $f_3 = \sin\Theta(\cos\Psi + \sin\Psi)$; and

$F_{11} = 2 \sin\Theta \sin\Phi[\cos\Psi \cos\Phi(\cos\Psi - \sin\Psi) - \sin\Phi \cos\Theta(\cos\Psi + \sin\Psi)]$,

$F_{22} = 2 \sin\Theta \cos\Phi[\sin\Phi(\cos\Psi - \sin\Psi) + \cos\Theta \cos\Phi(\cos\Psi + \sin\Psi)]$,

$F_{33} = 2 \cos\Theta \sin\Theta(\sin\Psi + \cos\Psi)$,

$$F_{13} = \sin\Phi(\cos\Psi + \sin\Psi)[\cos^2\Theta - \sin^2\Theta] + \cos\Theta\cos\Phi(\cos\Psi + \sin\Psi),$$
$$F_{23} = \cos\Theta[\sin\Phi(\cos\Psi - \sin\Psi) + \cos\Phi\cos\Theta(\cos\Psi + \sin\Psi)] - \sin^2\Theta\cos\Phi[\cos\Psi + \sin\Psi],$$
$$F_{12} = \sin\Theta(\cos\Psi - \sin\Psi).$$

Next, let us discuss the case of interphase conversion in the ferroelectric ceramic. It is known[15] that the tetragonal (T) and rhombohedral (R) ferroelectric phases coexist in the PZT system for compositions near the MPB. According to SEM, SAED and TEM results, the domain structure in PZT ceramics with compositions near the MPB consists of alternating T and R phase layers which resemble the 90° domain structure in tetragonal distorted ceramics. Based on experimental results, Lucuta proposed[19,20] a layered model of ferroelectric domains $T_1RT_2RT_1$, assuming the R domains are in between two different oriented T domains as shown in Figure 2. With a rhombohedral phase in between two 90° tetragonal domains, the polarization direction changes as follows: [001]---[111]---[010]---[111]---[001], corresponding to a repetitive domain sequence $T_1RT_2RT_1\ldots$. The interphase boundary conversion will induce changes in the electric and elastic dipole moments. As an example, when the polarization along the [111] direction in a R domain is switched into the polarization along the [001] direction in a T domain, the induced electric and elastic dipole moments in the primed coordinate system are:

$$\delta\vec{P}' = \Delta l A \frac{P_0}{\sqrt{3}} \begin{bmatrix} 1 \\ 1 \\ -(\sqrt{3}-1) \end{bmatrix} \tag{8}$$

$$\delta\tilde{U}' = \Delta l A \begin{bmatrix} u_{11} & u_{12} & u_{13} \\ u_{21} & u_{22} & u_{23} \\ u_{31} & u_{32} & u_{33} \end{bmatrix} \tag{9}$$

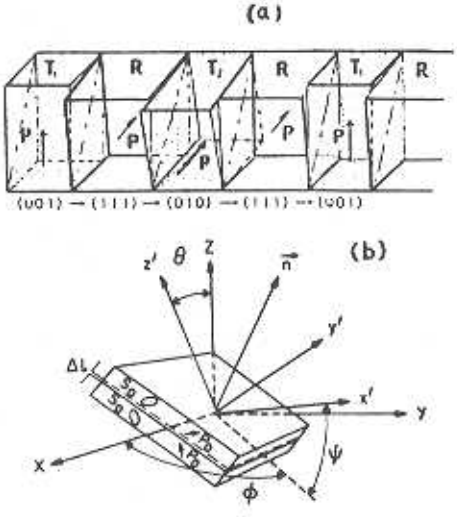

FIGURE 2 (a) Packing model of T-R twin-related domains along the (011) habit plane showing the coexistence of T and R ferroelectric phases in PZT at the MPB [After Lucuta Reference 20]. (b) A basic element of the interphase boundary in the PZT system at the MPB.

where,

$$u_{12} = u_{13}u_{21} = u_{23} = u_{31} = u_{32} = \frac{Q_{44}}{3} P_0^2;$$

$$u_{11} = u_{22} = \frac{(Q_{11} - Q_{12})}{3} P_0^2; \qquad u_{33} = \frac{-2(Q_{11} + Q_{12})}{3} P_0^2$$

Note: here we assume that the magnitude of the spontaneous polarization in the rhombohedral phase is equal to that in the tetragonal phase, and all coefficients Q_{11}, Q_{12}, and Q_{44} are the same in both phases. Finally, in the (x, y, z) coordinate system, the changes of electric and elastic dipole moments can be written as:

$$\delta P_i = [\widetilde{R}_{ij}][\delta P_i']; \qquad [\delta U_{ij}] = [\widetilde{R}_{ij}][\delta U_{ij}'][R_{ij}] \tag{10}$$

$$[R_{ij}] = \begin{bmatrix} \cos\Psi & \sin\Psi & 0 \\ -\sin\Psi & \cos\Psi & 0 \\ 0 & 0 & 1 \end{bmatrix} \begin{bmatrix} 1 & 0 & 0 \\ 0 & \cos\Theta & \sin\Theta \\ 0 & -\sin\Theta & \cos\Theta \end{bmatrix} \begin{bmatrix} \cos\Phi & \sin\Phi & 0 \\ -\sin\Phi & \cos\Phi & 0 \\ 0 & 0 & 1 \end{bmatrix}$$

2.2. *The Model*

Generally speaking, the domain wall motion is accomplished by a succession of steps beginning at initiating nuclei,[36,37] but in the sideways motion of the non-180°, this may not be exactly true.[38] The entire ceramic specimen is a complex electromechanical system with the domain walls in different grains having different orientations and different boundary conditions. The movements of the domain walls are not independent; there are strong interactions between them. The microscopic process for individual domain wall motion is rather complicated and not well understood. However, if we are only interested in the macroscopic effects resulting from the collective motion of domain walls, the microscopic details of each individual domain may be neglected.

In this analysis, we assume that the average displacement of a domain wall in a certain direction is quasi-one dimensional, i.e., the wall moves as a plane without bending. Figure 3 shows the variation of the wall energy as a function of position

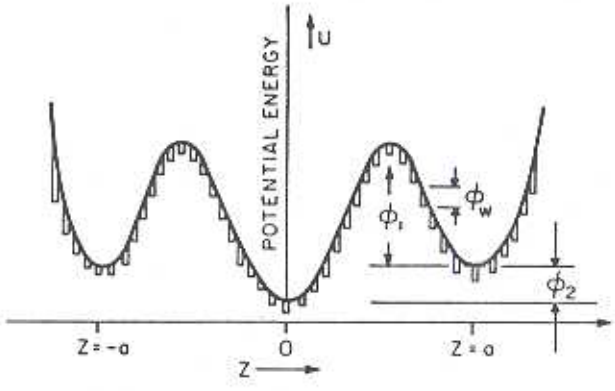

FIGURE 3 Schematic plot of the energy potential for non-180° domain wall motion in PZT ceramics.

in a ceramic sample. The height of the potential barrier ($\Phi_1 + \Phi_2$) is the minimum energy required for the wall to relocate from a depoling state to the poled state. Φ_w is the height of potential barrier for a non-180° domain wall going across one lattice distance.

In a depolarized ceramic sample, all domain walls are randomly oriented, and the distribution of domain walls possesses the symmetry of $\infty\infty m$. Obviously, domain walls are located at the minima of the potential energy ($z = 0$).

When an external ac field is applied, the domain walls oscillate. However, as long as the magnitude of the domain wall vibration is not very large, the macroscopic potential energy for domain wall motions is symmetric with respect to the z axis, i.e. $U(\Delta z) = U(-\Delta z)$. The situation is different for a poled ceramic. During the poling process, the domain walls overcome certain energy barriers, and move into new equilibrium positions. As shown in Figure 3, the new positions are metastable states ($z = a$, or $z = -a$). After the field is removed, the orientation distribution of the domain walls becomes conical in the poled samples. The potential for domain wall motion is no longer symmetric in the poled state, i.e. $U(a - \Delta z) \neq u(a + \Delta z)$.

It also has been shown[39,40] experimentally that the domain wall motion in a poled ceramic is highly nonlinear. Therefore, the potential energy for the domain wall motion may be expanded as a polynomial function of the domain wall displacement[33]:

$$u = U_0 + \frac{C_1}{2}\Delta l^2 + \frac{C_2}{3}\Delta l^3 + \frac{C_3}{4}\Delta l^4 + \text{higher-order terms} \tag{11}$$

where U_0 is the residual energy of a domain boundary, which is assumed to be independent of the domain wall motion. The presence of the third power term describes the asymmetric feature of the domain wall motion in a ferroelectric ceramic. The odd terms will be zero if domain wall vibrations take place around a potential energy minimum of the domain wall. Therefore, the differential equation of the forced vibration of a non-180° domain wall in a ferroelectric ceramic may be expressed as follows[13,14,38]:

$$Am\ddot{\Delta l} + Ab\dot{\Delta l} + \frac{\partial U}{\partial \Delta l} = -\left(\frac{\partial W_E}{\partial \Delta l} + \frac{\partial W_M}{\partial \Delta l}\right) \tag{12}$$

where m represents the effective mass of the domain wall, b is the damping constant, and the dots on top of Δl represent the derivatives with respect to time. The third term is the restoring force. W_E and W_M are the energies of the average electric and elastic dipoles $\langle \delta P_i \rangle$ and $\langle \delta U_{ij} \rangle$ induced by the electric field and stress, respectively, which may be written as

$$-(W_E + W_M) = \left(\sum \langle \delta P_i \rangle E_i e^{j\omega_1 t} + \sum \langle \delta U_j \rangle T_j e^{j\omega_2 t}\right) \tag{13}$$

In general, the electric and elastic driving frequencies are different, $\omega_1 \neq \omega_2$. The physical origins of the restoring force, damping effects and effective mass have

been discussed separately by several scientists.[36-45] If we consider only the first three terms of the restoring force, Equation (12) becomes

$$Am\Delta\ddot{l} + Ab\Delta\dot{l} + AC_1\Delta l + AC_2\Delta l^2 + AC_3\Delta l^3 = -\left(\frac{\partial W_E}{\partial \Delta l} + \frac{\partial W_M}{\partial \Delta l}\right) \quad (12')$$

This equation describes the interrelationship between the amplitude of the non-180° domain wall vibration and the stiffness of the materials. The condition

$$C_1\Delta l >> C_2\Delta l^2,\ C_3\Delta l^3$$

allows one to employ a perturbation method[46] in solving Equation (12'). Approximate values can be obtained for the induced polarization δP_i and strain δU_{ij} resulting from the motion of non-180° domain walls. The detailed solutions are presented in Reference 33. According to Fousek and Brezina,[38] the resonant frequency of domain walls is much higher than the frequencies used in our experiments, which are less than 1 MHz. Thus, the inertia term can be neglected. This means that the damping is sufficiently strong that Equation (12') can be simplified to a relaxation equation.

III. LINEAR AND NONLINEAR COEFFICIENTS

We now consider the linear and nonlinear dielectric, piezoelectric, and elastic properties associated wth the 110° domain wall motion in ferroelectric ceramics. The average induced polarization and strain can be calculated by averaging δU_{ij} and δP_i over all domain wall orientations in the sample.[13,14] $\Delta P_i = \langle \delta P_i \rangle$, and $\Delta U_{ij} = \langle \delta U_{ij} \rangle$ may be expressed as:

$$\begin{aligned}
\Delta P_i &= [\Delta\varepsilon_{ik} + \Delta r_{ijk}E_j]E_k + [\Delta d_{im} + \Delta e_{ilm}T_l]T_m + 2\Delta Q_{ijl}E_jT_l \\
&\quad + \Delta H_{ijkp}E_jE_kE_p + \Delta G_{ijkl}E_jE_kT_l + \ldots \\
\Delta U_l &= [\Delta d'_{jl} + \Delta Q'_{ijl}E_i]E_j + [\Delta S_{ln} + \Delta S_{lmn}T_m]T_n + 2\Delta e'_{lkm}E_kT_m \qquad (14) \\
&\quad + \Delta G'_{ijkl}E_iE_jE_k + \Delta W_{ijnl}E_iE_jT_n + \ldots \\
&\quad (i, j, k, p = 1, 2, 3 \text{ and } l, n, m = 1, 2, 3, 4, 5, 6)
\end{aligned}$$

In these expressions, ΔP_i is the total induced average polarization, and ΔU_l is the average strain component in Voigt notation, T_n is the stress, and E_k is the electric field and the expansion coefficients are defined below. The coefficients $\Delta d_{kl} = \langle \delta d_{kl} \rangle$ are the extrinsic piezoelectric constants of a ceramic sample:

$$\Delta d_{kl} = \int_0^{2\pi} d\phi \int_0^{2\pi} d\psi \int_0^{\pi} \frac{1}{\sqrt{3}} S_0P_0K(\omega_i)f_kF_iZ(\Theta)\, d\Theta \qquad (15)$$

where

$F_1 = F_{11}, F_2 = F_{22}, F_3 = F_{33}, F_4 = F_{23}, F_5 = F_{13}, F_6 = F_{12}$, and,

$$K(\omega_i) = \int_0^{\infty} \frac{Ag(\tau)\, d\tau}{C_i(1 + j\omega_i\tau)}$$

Note: Δd_{kl} depends on ω_2, the frequency of the applied elastic field, and $\Delta d'_{kl}$ depends on ω_1, the frequency of the applied electric field. $g(\tau)$ is the relaxation time distribution[13,14] assuming there exists more than one relaxation time. $Z(\Theta)$ is the distribution function of domain wall orientations obtained during the poling process. All quantities having the Δ symbol are caused by 110° domain wall vibrations only. The values of $\Delta s_{lm} = \langle \delta s_{lm} \rangle$ and $\Delta \varepsilon_{ik} = \langle \delta \varepsilon_{ik} \rangle$ are the extrinsic elastic and dielectric parameters of the ceramic:

$$\begin{aligned} \Delta s_{lm} &= \int_0^{2\pi} d\phi \int_0^{2\pi} d\psi \int_0^{\pi} S_0^2 K(\omega_2) F_l F_n Z(\Theta)\, d\Theta \\ \Delta \varepsilon_{ik} &= \int_0^{2\pi} d\phi \int_0^{2\pi} d\psi \int_0^{\pi} \frac{1}{3} P_0^2 K(\omega_1) f_i f_k Z(\Theta)\, d\Theta \end{aligned} \tag{16}$$

where $\Delta Q_{ijl} = \langle \delta Q_{ijl} \rangle$ (electrostrictive coefficients) and $\Delta r_{ijk} = \langle \delta r_{ijk} \rangle$ (nonlinear dielectric coefficients) can be expressed as follows:

$$\begin{aligned} \Delta Q_{ijl} &= \int_0^{2\pi} d\phi \int_0^{2\pi} d\psi \int_0^{\pi} \frac{-2}{3} S_0 P_0^2 K'(\omega_1, \omega_2) f_i f_j F_l Z(\Theta)\, d\Theta \\ \Delta Q'_{ijl} &= \int_0^{2\pi} d\phi \int_0^{2\pi} d\psi \int_0^{\pi} \frac{-2}{3} S_0 P_0^2 K'(\omega_1) f_i f_j F_l Z(\Theta)\, d\Theta \end{aligned} \tag{17}$$

where

$$K'(\omega_1) = \int_0^{\infty} \frac{C_2 A g(\tau)\, d\tau}{4C_1(1 + 2j\omega_1\tau)(1 + j\omega_1\tau)^2};$$

$$K'(\omega_1, \omega_2) = \int_0^{\infty} \frac{C_2 A g(\tau)\, d\tau}{4C_1(1 + j[\omega_2 + \omega_1]\tau)(1 + j\omega_1\tau)(1 + j\omega_2\tau)}.$$

and

$$\Delta r_{ijk} = \int_0^{2\pi} d\phi \int_0^{2\pi} d\psi \int_0^{\pi} -2P_0^3 K'(\omega_1) f_i f_k f_k Z(\Theta)\, d\Theta \tag{18}$$

Here, we should point out that the contributions of domain wall motion to the electrostrictive coefficients ΔQ_{ijl} and the nonlinear dielectric coefficients Δr_{ijk} have the same physical origin as those of the electro-optical coefficients and elasto-optical coefficients. In fact, in hot pressed transparent PLZT ceramics the changes of the remnant polarization give rise to changes in the birefringence Δn[47-50] because of the non-180° domain reversal induced by an external field.

The electroacoustic coefficients $\Delta e_{klm} = \langle \delta e_{klm} \rangle$ (the coefficients of the nonlinear piezoelectric effect) describe the change in the velocity of elastic waves, and are given by:

$$\begin{aligned} \Delta e'_{klm} &= \int_0^{2\pi} d\phi \int_0^{2\pi} d\psi \int_0^{\pi} \frac{-2}{\sqrt{3}} P_0 S_0^2 Z(\theta) K'(\omega_2) f_k F_l F_m\, d\theta \\ \Delta e_{klm} &= \int_0^{2\pi} d\phi \int_0^{2\pi} d\psi \int_0^{\pi} \frac{-2}{\sqrt{3}} P_0 S_0^2 Z(\theta) K'(\omega_1, \omega_2) f_k F_l F_m\, d\theta \end{aligned} \tag{19}$$

In some materials,[7] the extrinsic contribution to the electroacoustic effect (change

in velocity of sound under an applied electric field) may be two orders of magnitude larger than the intrinsic contribution. The third order elastic coefficients $\Delta S_{lmn} = \langle \delta S_{lmn} \rangle$ are:

$$\Delta S_{lmn} = \int_0^{2\pi} d\phi \int_0^{2\pi} d\psi \int_0^{\pi} -S_0^3 Z(\Theta) K'(\omega_2) F_l F_m F_n \, d\Theta \tag{20}$$

There are twenty one non-vanishing coefficients. The expressions for the higher order nonlinear piezoelectric coefficients $\Delta G_{ijkl} = \langle \delta G_{ijkl} \rangle$ and dielectric coefficients $\Delta H_{ijkp} = \langle \delta H_{ijkp} \rangle$ are given by the following integrals:

$$\begin{aligned} \Delta G'_{ijkl} &= \int_0^{2\pi} d\phi \int_0^{2\pi} d\psi \int_0^{\pi} \frac{1}{3\sqrt{3}} S_0 P_0^3 K''(\omega_1) f_i f_j f_k F_l Z(\Theta) \, d\Theta \\ \Delta G_{ijkl} &= \int_0^{2\pi} d\phi \int_0^{2\pi} d\psi \int_0^{\pi} \frac{1}{3\sqrt{3}} S_0 P_0^3 K''(\omega_1, \omega_2) f_i f_j f_k F_l Z(\Theta) \, d\Theta \end{aligned} \tag{21}$$

Where

$$\begin{aligned} K''(\omega_1) &= \int_0^{\infty} \left\{ \frac{C_2^2 A g'(\tau)}{4C_1^5 (1 + 2j\omega_1\tau)(1 + 3j\omega_1\tau)(1 + j\omega_1\tau)^3} \right. \\ &\qquad \left. - \frac{C_3 A g'(\tau)}{4C_1^4 (1 + 3j\omega_1\tau)(1 + j\omega_1\tau)^3} \right\} d\tau \\ K''(\omega_1, \omega_2) &= \int_0^{\infty} \left(\frac{C_2^2 A g'(\tau)(1 + j\omega_1\tau)^{-2}}{4C_1^5 (1 + 2j\omega_1\tau)(1 + j[2\omega_1 + \omega_2]\tau)(1 + j\omega_2\tau)} \right. \\ &\qquad \left. - \frac{C_3 A g'(\tau)(1 + j\omega_1\tau)^{-2}}{4C_1^5 (1 + j[2\omega_1 + \omega_2]\tau)(1 + j\omega_2\tau)} \right) d\tau \end{aligned}$$

and

$$[\Delta H_{ijkp}] = \int_0^{2\pi} d\phi \int_0^{2\pi} d\psi \int_0^{\pi} \frac{1}{9} P_0^4 K''(\omega_1) f_i f_j f_k f_p Z(\Theta) \, d\Theta \tag{22}$$

Note that all the quantities are frequency dependent. When electric and elastic fields are applied simultaneously with different frequencies, one finds the direct and converse effects have different magnitude, for example, if $\omega_1 \neq \omega_2$, $\Delta d_{kl}(\omega_1) \neq \Delta d_{kl}(\omega_2)$, therefore, we have used a prime on some of the constants in ΔU_i to indicate their frequency dependence. In general, the contributions from 71°, 110° and 90° twin structures can be all written in the form of Equation (14)–Equation (22) except that the integration coefficients would be different in each case.

If $T_l = 0$, Equation (14) becomes:

$$\begin{aligned} \Delta P_i &= \Delta \varepsilon_{ik} E_k + \Delta r_{ijk} E_j E_k + \Delta H_{ijkp} E_j E_k E_p \\ \Delta U_i &= \Delta d_{kl} E_k + \Delta Q_{ikl} E_i E_k + \Delta G_{ijkl} E_i E_j E_k \\ & \qquad i, j, k, l, p = 1, 2, 3 \end{aligned} \tag{23}$$

The electric field induced longitudinal strain and polarization arising from the domain wall motion are:

$$\begin{aligned} \Delta U_3 &= \Delta d_{33} E_0 + \Delta Q_{333} E_0^2 + \Delta G_{3333} E_0^3 \\ \Delta P_3 &= \Delta \varepsilon_{33} E_0 + \Delta r_{333} E_0^2 + \Delta H_{3333} E_0^3 \end{aligned} \tag{24}$$

Similarly, the shear strain and related polarization under the applied a.c. electric field are described by:

$$\begin{aligned} \Delta U_5 &= \Delta d_{15} E_0 + \Delta G_{1115} E_0^3 \\ \Delta P_1 &= \Delta \varepsilon_{11} E_0 + \Delta H_{1111} E_0^3 \end{aligned} \tag{25}$$

There are no second harmonic and higher even harmonic components in shear vibrations. Therefore, it is expected that the dependence of Δd_{15} and $\Delta \varepsilon_{11}$ on the alternating electric field strength should have different characteristics than those of Δd_{33}, Δd_{31}, and $\Delta \varepsilon_{33}$.

Strictly speaking, under external forces the difference in free energy for the two domains of a twin is[51]:

$$\Delta g = \Delta \varepsilon_{(s)ij} \sigma_{ij} + \Delta P_{(s)i} E_i + \frac{1}{2} \Delta s_{ijkl} \sigma_{ij} \sigma_{kl} + \frac{1}{2} \Delta \kappa_{ij} E_i E_j + \Delta d_{ijk} E_i \sigma_{jk} \tag{26}$$

where, the first two terms are the differences of the spontaneous strain and polarization of the two domains, which is primary ferroic effect. The remaining three terms in Δg arise from external force induced differences in elastic compliance, dielectric susceptibility, and piezoelectric coefficients, which represent the secondary ferroic behavior. In this paper, only the primary ferroic effect is discussed. Based on this viewpoint, it could be found that the extrinsic properties of a twin structure arise from the orientational differences in their intrinsic properties. External forces or fields induce the differences in free energy for the two domains, causing domain walls to move, and creating the extrinsic contributions.

IV. EXPERIMENTAL RESULTS AND DISCUSSIONS

4.1. Experimental Procedure

Several compositions of the PZT solid solution system were selected for this study. The ceramic $Pb(Zr_xTi_{1-x})O_3$ specimens with $x = 0.90, 0.70, 0.60, 0.54, 0.52, 0.50, 0.40, 0.30$, and 0.15 were prepared by a conventional mixed oxide technique. The starting materials of PZT material are also included, both the powders made by the sol-gel method and the $Pb(Zr_{0.52}Ti_{0.48})O_3$ + (0.4 – 0.8% wt. Nb_2O_3) powders. Well sintered ceramic samples were poled at an electric field of 30–65 kV/cm in the temperature range of 100°C–130°C. These poled samples were first checked with a commercial Berlincourt d_{33} meter. Values of the piezoelectric coefficients are listed in Table I. In addition, some ceramic samples, PZT-501A and PZT-401 which were made by commercial powders form the Ultrasonic Powders Inc., South Plainfield, NJ. And also several of the hard and soft PZT specimens, PZT-5, PZT-

TABLE I

Piezoelectric coefficients for $Pb(Zr_xTi_{1-x})O_3$ ceramics. The measurements were made by the commercial Berlincourt meter

Zr/Ti.	90/10	70/30	60/40	54/46	52/48	50/50	40/60	30/70	15/85
Density (10^3 kg/m^3)	7.44	7.55	7.60	7.62	7.7	7.4	7.6	7.59	7.3
d_{33} (10^{-12} m/V)	?	85-100	100-120	170-200	250-270	100-120	90-100	50-60	?

8 and PZT-4 used in this study are commercial products from Vernitron piezoelectric division, Bedford, OH.

Permittivity-temperature runs were made in a computer-controlled environmental chamber (Delta Design Model 2300) using liquid nitrogen as a cooling agent. Both heating and cooling rates are about 5°C/min. Data were recorded with a digital multimeter controlled by a desk top computer system (Model 9816, Hewlett Packard Inc.). The dielectric response of the sample was measured by using a modified Sawyer-Tower circuit and a precision capacitance meter (HP 4275A Multi-Frequency LCR Meter). The piezoelectric coefficients were measured by both optical interferometry and iterative methods.[53,54] The resonance-antiresonance method is widely used for measuring piezoelectric coefficients in weak electric fields at which the vibrating system remains linear. However, when the amplitude of the applied field becomes very large, the resonance-antiresonance method is no longer suitable due to the nonlinearity. Therefore, an interferometry technique was used for measurements under large alternating electric fields. The advantages of the interferometry, apart from its directness, are the simplicity in computational expressions. In addition, the measurements can be carried out under both resonance and non-resonance conditions and are not limited by the amplitude of the external fields. Moreover, a wide range of sample shapes and sizes can be tolerated. The HP4192 A LF impedance analyzer was used when employing the resonance technique which has been standardized by IEEE.[53] In measuring the nonlinear parameters, a sinusoidal driving field was used for convenience of interpretation. Resistive tunable low-pass active-filters were used (Package Date 730/740 Series, Frequency Devices, Inc.) in the measurement system. Samples were made as thin as possible in order to achieve a high field with low voltage. For larger displacements, Equation (2) of Reference 54 is no longer valid, and the cosine term in Equation (3) of Reference 54 must be expanded using the Fourier-Bessel expansion. It is important to realize that the nonlinear output signals may be caused by either the nonlinearity of materials or by the distortion of the input signal in the detecting system. There are two ways to avoid the detecting system producing nonlinear output signals. (1) Using the quartz as the pre-calibration sample, we can retrieve the actual measured experimental data in order to remove the nonlinear contribution of the detecting system. (2) Through keeping the thickness of the samples down, we can get sufficiently large strains while restricting the maximum displacement of the sample to values less than 140 Å.

4.2. *Results and Discussions*

A. *Nonlinear piezoelectric and dielectric coefficients.* Figure 4 shows the piezoelectric constants d_{kl} and the dielectric constants ε_{ii} plotted as a function of applied a.c. field strength. When the magnitude of the applied electric field is below a certain limiting value E_t (called the threshold field), d_{kl} and ε_{ii} remain constant. But beyond the threshold field ($E > E_t$), d_{lk} and ε_{ij} increase with the amplitude of the a.c. electric field. E_t signifies the onset of measurable nonlinearity, which is not always clearly defined. We use $\Delta d/d$ $(\Delta\varepsilon/\varepsilon) > 2.5\% - 4\%$ as the criteria according to different experimental conditions. Generally, E_t depends on frequency, temperature and material properties. For instance, for PZT-501A with F = 200 Hz and T = 25°C, the threshold field for the piezoelectric coefficient d_{33} is approximately 300 V/cm. Analogously, when the applied field exceeds a certain value, dielectric losses also increase drastically with the amplitude of a.c. electric field,[33] but the threshold fields for the loss seem to be smaller than those for the dielectric and piezoelectric coefficinets. By using an oscilloscope to follow the polarization (P) and strain (S) under a.c. electric field (E) at a given frequency, it was found that the P and S vs. E curves are straight lines for small oscillation amplitudes, but the average slope of the hysteresis increases rapidly when the amplitude of the a.c. field exceeds certain values, as shown in the insertion of Figure 4. Since the non-180° domain wall motion is inherently a lossy process,[55–57] the strong correlation between loss and nonlinearity suggests that electromechanical nonlinearity in ferroelectric ceramics originates mainly from the

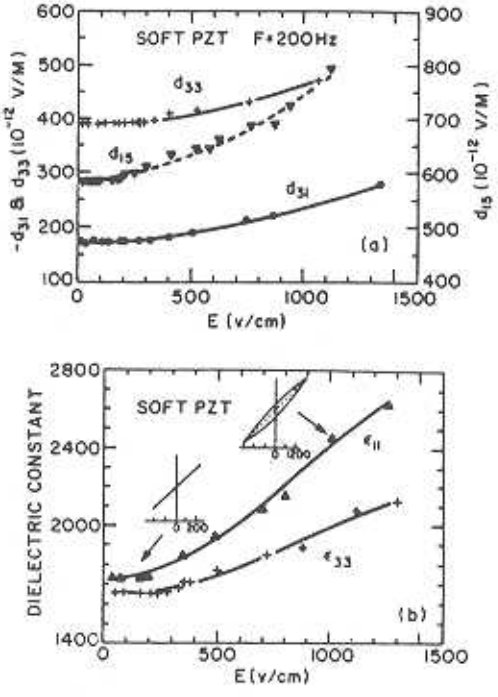

FIGURE 4 (a) a.c. electric field dependence of the piezoelectric coefficients d_{31}, d_{33}, and d_{15}. (b) a.c. electric field dependence of dielectric coefficients ε_{11}, and ε_{33}.

motion of non-180° domain walls. Spectrum analyses were made to identify the higher harmonic components in the responses of polarization and strain. It is found[33] that when the direction of a.c. field is perpendicular to the poling direction of the sample, only odd harmonics exist and the shape of the hysteresis loops (both for strain and polarization vs. a.c. electric field) is always symmetric. On the other hand, when an a.c. electric field E is parallel to the poling direction, both odd and even harmonics exist. They become obvious when external field is above the certain level. The shape of hysteresis loop is no longer symmetric. This may be understood from Equations (24) and (25). Assuming $E_{ac} = E_0 \cos \omega t$, from Equation (23), the longitudinal strain is:

$$\Delta U_3 = \Delta d_{33} E_{ac} + \Delta r_{333} E_{ac}^2 + \Delta G_{3333} E_{ac}^3 = Y_0 + Y_1 e^{j\omega t} + Y_{-1} e^{-j\omega t} + Y_2 e^{2j\omega t} + Y_{-2} e^{-2j\omega t} + Y_3 e^{3j\omega t} + Y_{-3} e^{-3j\omega t} + \ldots \quad (27)$$

where

$$Y_0 = \Delta r_{333} \frac{E_0^2}{2}; \qquad Y_1(\omega) = Y_{-1}(-\omega) = \left(\Delta d_{33} E_0 + \frac{3 \Delta G_{3333} E_0^3}{4} \right)$$

$$Y_2(\omega) = Y_{-2}(-\omega) = \Delta r_{333} \frac{E_0^2}{2}; \qquad Y_3(\omega) = Y_{-3}(-\omega) \frac{\Delta G_{3333} E_0^3}{4}$$

The term $(Y_n e^{jn\omega t} + Y_{-n} e^{-jn\omega t})$ represents the component of the nth harmonic oscillation. Based on Equation (27), we would like to elaborate a few points:

1. The third order term increases the amplitude of the fundamental frequency by an amount of $3\Delta G_{3333} E_0^3/4$.
2. The second order harmonic term creates an additional negative bias field which displaces the center of vibration of the domain wall.
3. Both the second and the third harmonic vibrations of non-180° domain walls contribute to the induced longitudinal strain. This implies that the hysteresis loops of both P vs. E, and S vs. E should be asymmetric when the a.c. field is beyond the certain level. The situation is somewhat different for the shear strain. From Equation (23), we have

$$\Delta U_5 = \Delta d_{15} E_{ac} + \Delta G_{1115} E_{ac}^3 = Y_0 + Y_1 e^{j\omega t} + Y_{-1} e^{-j\omega t} + Y_3 e^{3j\omega t} + Y_{-3} e^{-3j\omega t} + \ldots \quad (28)$$

where

$$Y_0 = 0; \qquad Y_1(\omega) = Y_{-1}(-\omega) = \Delta d_{15} E_0 + \frac{3 \Delta G_{1115} E_0^3}{4}$$

$$Y_2(\omega) = Y_{-2}(-\omega) = 0; \qquad Y_3(\omega) = Y_{-3}(-\omega) = \frac{\Delta G_{1115} E_0^3}{4}$$

There is no second harmonic in the shear strain, which is in agreement with the experimental results. Measurements of the complex ε_{ij} have been carried out with doped PZT ceramics. Figure 5 shows the relative dielectric permittivity ε_{11} and ε_{33} of the PZT-5 ceramic as well as their loss tangents as a function of temperature from −200°C to 50°C at two different magnitudes of the applied a.c. electric field. Figure 6 shows the dielectric permittivity ε_{33} and its loss versus temperature at different a.c. electric field strengths. Clearly, the values of ε_{11} and ε_{33} as well as

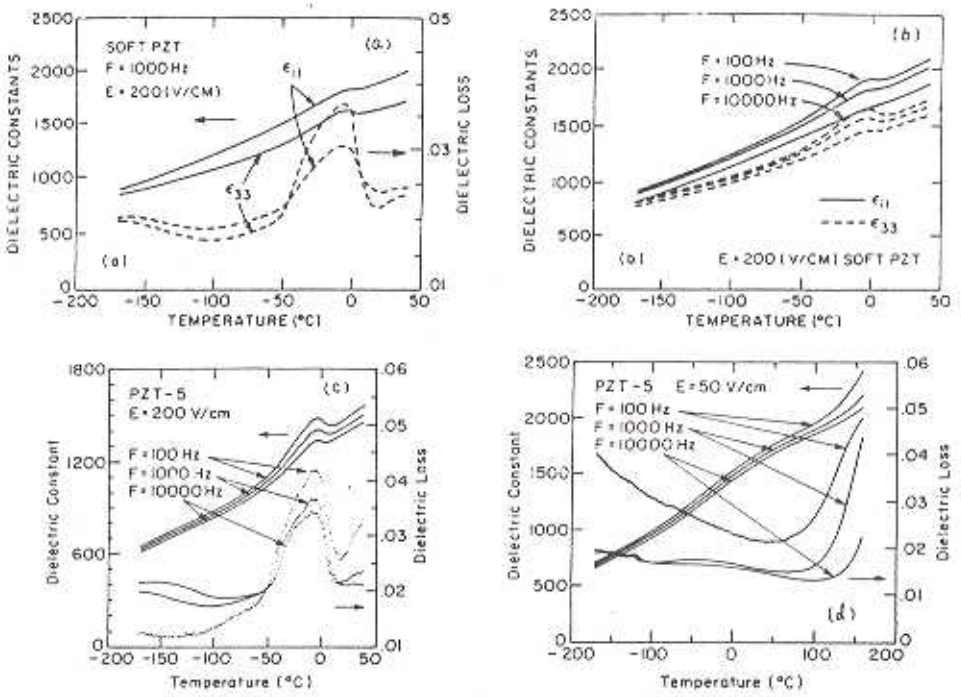

FIGURE 5 (a) ε_{11} and ε_{33} and their losses as a function of temperature for a PZT-501A sample. (b) The values of ε_{11} and ε_{33} as a function of temperature for PZT-501A at different frequencies. (c) and (d) are the temperature dependence of dielectric constant ε_{33} and its loss for a PZT-5 ceramic measured at the field levels of 200 V/cm and 50 V/cm, respectively, at three different frequencies.

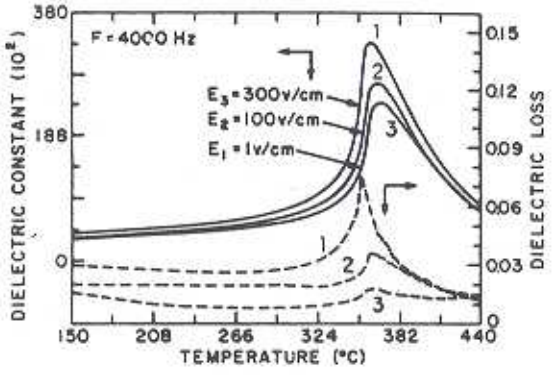

FIGURE 6 Temperature dependence of ε_{33} and its tan δ of a PZT-501A sample at different magnitudes of a.c. fields.

their losses are quite different at high temperatures, these differences become smaller as temperature decreases. This may reveal that part of the difference between ε_{11} and ε_{33} may come from the domain boundary vibrations which are frozen out at very low temperatures. It is found that PZT with composition near the morphotropic boundary has one relaxation region in the low temperature regime, which has been also observed by others.[13] The interesting thing is that under

a.c. external field, a pseudo relaxation peak can be observed (Figure 5(c)) in a very broad frequency range, which can be interpreted as the "clamping" of the large magnitude movement of domain walls. In Reference 33, it has been shown that the threshold fields of the piezoelectric coefficients increase with aging time, which is another strong implication that the threshold field is closely related to non-180° domain wall motion, because the reduction of the non-180° domain wall mobility is responsible for the aging phenomena in ferroelectric ceramics.[58] It is also found[33] that the threshold field strengths of the dielectric and piezoelectric coefficients decrease with increasing the magnitude of an applied positive d.c. bias field which provides the pinning to the wall motion. The nonlinearity also decreases with temperature due to the fact that the domain wall becomes less mobile at lower temperature. Figure 7 shows the distribution of threshold fields for the piezoelectric coefficients of the PZT system with different compositions and dopants. A pronounced minimum value for the threshold field is found for the composition near the morphotropic phase boundary (MPB), which reveals that the domain walls have the highest mobility for compositions at the MPB. In second order approximation, the extrinsic contributions to the piezoelectric coefficient is given in Equation (23):

$$d_{kl} = \Delta d_{kl} + \Delta Q_{ikl}E_i + \Delta G_{ijkl}E_iE_j \tag{29a}$$

Assuming the nonlinearity is purely extrinsic, one has:

$$\langle d_{kl}\rangle = d_{kl(in)} + \Delta d_{kl} + \Delta Q_{ikl}E_i + \Delta G_{ijkl}E_iE_j \tag{29b}$$

where $\langle d_{ik}\rangle$ is the measured piezoelectric coefficient, which include both the intrinsic contribution, $d_{ik(in)}$, and the extrinsic contribution, the contribution, Δd_{ik}. Based on the definition of threshold field strength of $\langle d_{ik}\rangle$ described earlier, we have:

$$\left|\frac{\langle d_{33}\rangle - (d_{33(in)} + \Delta d_{33})}{(d_{33(in)} + \Delta d_{33})}\right|_{E_t} = \frac{\Delta Q_{333}E_t}{d_{33(in)} + \Delta d_{33}} \geqslant 3\% \tag{29c}$$

This means that the threshold field is inversely proportional to the ratio between the electrorestrictive coefficient and the piezoelectric coefficient. From Equation (15) and Equation (17), it is found that $\Delta d_{33}/\Delta Q_{333}$ is proportional to $(C_1)^2/(P_0C_2)$.

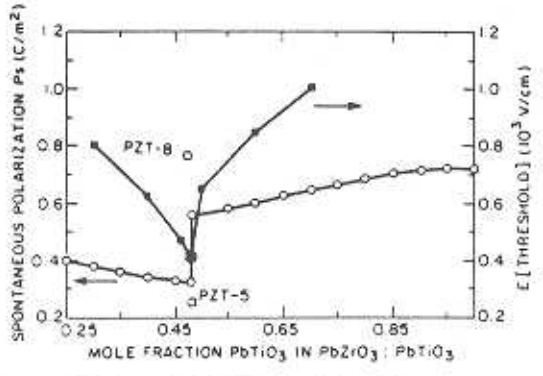

FIGURE 7 Dependence of the threshold field strength and the spontaneous polarization on the Ti/Zr ratio for PZT ceramics.

In Reference 41, the restoring force constant was estimated to be greater than the square of the spontaneous strain $C_1 > (S_0)^2$, and also $C_1 > C_2$. Therefore, $(\Delta d_{33}/\Delta Q_{333})$ can be estimated to be proportional to the spontaneous polarization. Thus from Equation (29c) one may conclude that the threshold field E_t should also increase with the spontaneous polarization. The experimental data in Figure 7 qualitatively shows this tendency. In addition, the threshold fields E_t for PZT-8 and PZT-4 are substantially higher than that of PZT-5 due to the influence of dopants on the domain wall mobility.

B. *Electromechanical nonlinearity under resonant frequency.* Many ultrasonic devices are operated at their resonance frequencies. When being driven at high field levels, the presence of nonlinearity alters the performance of these devices. In this section, we report some of the nonlinear effects under resonant conditions for a PZT-501A ceramic. Figure 8 shows the complex admittance circles at different drive levels. The outer circle (curve I) is measured at small-signal conditions, a field level of 1 V/cm. The system appears to be a typical linear piezoelectric resonator with very low loss. All the data points fall onto a perfect circle. The inner circle (curve II) was measured at a field level of 100 V/cm. One can see that the data points obviously deviate from the small circle showing the presence of nonlinearity.

This is expected from the measurements on piezoelectric effects because the relationship between d_{31} and field strength no longer remains linear under large field, invalidating the linear assumption made in the measurement technique. It is found that the magnitudes of $d_{31}[\mathrm{II}](-190 \times 10^{-12}$ V/m) and the loss tangent $d'_{31}[\mathrm{II}]/d_{31}[\mathrm{II}]$ (0.085), which were measured at high drive levels but non-resonant frequencies using an interferometer, are larger than those values ($d_{31}[\mathrm{I}] = -176 \times 10^{-12}$ V/m and $d'_{31}[\mathrm{I}]/d_{31}[\mathrm{I}] = 0.018$) measured at low driving levels. This strongly implies that the nonlinear effects at the resonance frequency are caused by the nonlinear increase in piezoelectric coefficients. We suggest that this nonlinear change in piezoelectric coefficients originates from the domain wall motion since the increase of the macroscopic-losses mainly arises from domain wall motions.[33] When the applied field exceeds a certain level, the nonlinear domain wall motions start to contribute to the piezoelectric effect, and the coupling between the vibrations

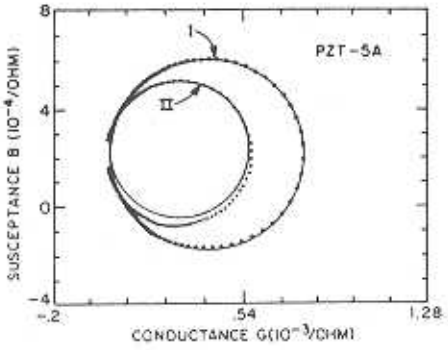

FIGURE 8 Complex admittance plot of PZT-501A bar measured with two different applied field strengths. Curve I: $E_1 = 1$ V/cm and curve II: $E_2 = 100$ V/cm.

of domain wall and extensional mode causes the nonlinear effects at the resonance frequency. The field dependence of the electromechanical properties causes the extremum frequencies of the admittance to shift as shown in Figure 9. Figure 9(a) is the amplitude of the admittance of a PZT-501A plate, which was measured with a spectrum analyzer. The resonant frequency f_m shifts towards lower frequencies with increasing applied a.c. voltage, but the anti-resonance frequencies f_n do not shift significantly as reported by Uchino *et al.*[6]

Interestingly, however, when measuring the absolute value of admittance $|Y|$ of a bar sample with an impedance analyzer, we found that both f_m and f_n shift noticeably to lower frequencies at higher driving level, as shown in Figure 9(b), which may imply that the nonlinearity affects certain vibration modes more severely than to the others. Meanwhile, the experimental results could be affected by the measurement techniques.

Figure 10 and Figure 11 show the dielectric losses and dielectric constants as a function of frequency, respectively, under different field levels near an isolated resonance. It can be seen that the resonance peaks of both the dielectric loss and the dielectric constant move toward lower frequencies at the high drive level. The

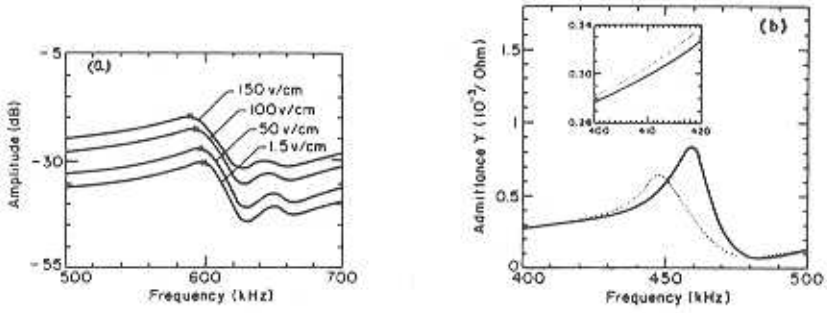

FIGURE 9 Typical admittance curves measured for the PZT-501A samples at different driving levels. (a) Measured electrical admittance of PZT-501A plate at four different driving levels. (b) Absolute value of admittance $|Y|$ for a PZT-501A bar at two driving levels. The solid line and the dash line represent results obtained at field levels of E_1 = 1 V/cm and E_2 = 100 V/cm respectively.

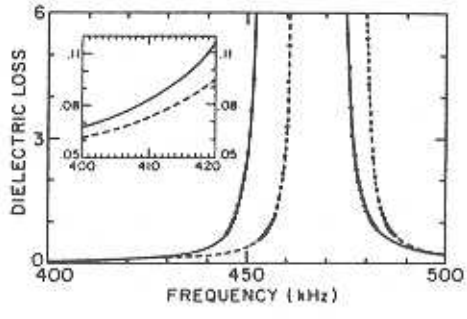

FIGURE 10 Dielectric losses vs frequency with respect to different driving levels for a PZT-501A bar in the vicinity of the resonance frequency. The dash line is for E_1 = 1 V/cm and the solid line is for E_2 = 100 V/cm.

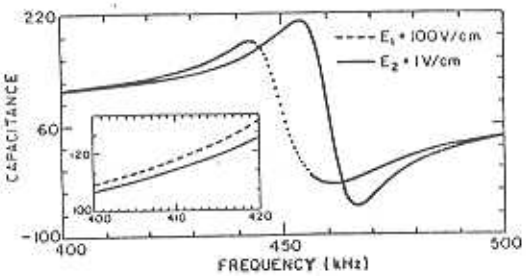

FIGURE 11 Capacitance of a PZT-501A bar vs. frequency in the vicinity of the resonance frequency at different driving levels.

dielectric loss in the vicinity of the resonant frequency also becomes larger for the case of higher drive level as shown in Figure 10. It should be noted that when large electric field is applied, nonlinear effects occur at all frequencies, hence, the dielectric loss, mechanical loss, dielectric constant, elastic constants, and piezoelectric coefficients become larger in all frequency ranges. Away from the resonance, the motions of non-180° domain walls are an important cause for the changes in the dielectric, elastic, and piezoelectric coefficients. At the resonant frequency, changes of these coefficients will profoundly lead to the shifts of the resonance and antiresonance frequencies, f_m and f_n. In addition, the mechanical quality factor Q_m and the electromechanical coupling factors K_i will also be affected. The factors controlling the shift of resonant frequency are important in ultrasonic engineering. From Reference 28, in second order approximation, the shift of the resonant frequency for extensional vibration of an electromechanically excited bar can be written as:

$$\delta\omega_r^D = -\left\{\frac{32[S_{111}^E]^2}{9\pi^2 S_{11}^E} + \frac{9S_{1111}^E}{32}\right\}\frac{\omega_r^D d_{31}^2 E^2 Q^2}{[S_{11}^E]^2 a^2} \tag{30}$$

where ω_r^D is the resonant frequency of the extensional mode for a linear system, s_{11}^E and s_{111}^E are the second and third order elastic compliance. The frequency of the P_3 maximum is also shifted by the electric field,

$$\delta\omega_r^P = -\left\{\frac{(\varepsilon_{333}^T)^2}{\varepsilon_{33}^T} + \frac{3\varepsilon_{333}^T}{4}\right\}\frac{\omega_r^P E^2 Q^2}{2\varepsilon_{333}^T a^2} \tag{31}$$

where ω_r^P is the small-signal resonance frequency, Q is the mechanical quality factor and a is the thickness of the sample. Equations (30) and (31) are for single domain and single crystal system. For ceramics, there exist additional shifts of the resonant frequencies by domain wall motion. From Equations (15)–(21) they can be expressed as:

$$\Delta\omega_r^D = -\left\{\frac{32[\Delta S_{111}]^2}{9\pi^2(S_{11(in)} + \Delta S_{11})} + \frac{9\Delta G_{1111}}{32}\right\}\frac{\omega_r^D(d_{31(in)} + \Delta d_{31})^2 E^2 Q^2}{(S_{11(in)} + \Delta S_{11})^3 a^2} \tag{32}$$

and

$$\Delta\omega_r^P = -\left\{\frac{[\Delta r_{333}]^2}{\varepsilon_{33(in)} + \Delta\varepsilon_{33}} + \frac{3\Delta H_{3333}}{4}\right\}\frac{\omega_r^P E^2 Q^2}{2(\varepsilon_{33(in)} + \Delta\varepsilon_{33})a^2} \tag{33}$$

Here $\varepsilon_{ij(in)}$, $d_{ik(in)}$, and $S_{nm(in)}$ are intrinsic properties. The total shift of these resonance frequencies are the sum of intrinsic and extrinsic contributions. The above analyses give rise to a relationship between the shifts of the maximum frequency and the damping constant (or losses), restoring force constants, as well as spontaneous polarization and strain. The results shown in Equations (30)–(33) may be used to qualitatively explain the experimental results.

The mechanical and electric responses of a piezoelectric material depends not only on its piezoelectric properties, but also on its elastic and dielectric parameters, according to the constitutive piezoelectric equations.[59] Therefore, a figure of merit of a piezoelectric material must include its elastic, dielectric and piezoelectric coefficients, which are defined as the electromechanical coupling factors (often called coupling coefficients). The coupling coefficient k is used as a characteristic index for the performance of a transducer. The value of k^2 is a measure of the magnitude of the transducer bandwidth. It is useful to clarify the extrinsic contribution to the electromechanical coupling coefficients and to understand how the domain wall movements influence the coupling coefficient. Figure 12 shows the measured field dependence of the coupling coefficient k_{31} and the mechanical quality factor Q_m. One can see that the coupling factor, and the mechanical losses increase with the increase of the magnitude of a.c. field. The correlation between the coupling factor and the loss factor indicates that the extrinsic contributions plays a very important role in terms of the electric-mechanical energy conversion in ferroelectric ceramic. It should noted that the coupling factor is dependent on the stress and strain level, which often show spatial variations.[60]

In the high temperature regime, for some PZT system, it is difficult to abstract information on domain wall contribution from the measurement of dielectric and piezoelectric coefficients for a PZT system.[3,59] The problem is that the conductivity of some PZT systems increases drastically at high temperatures just like in semiconductors. Thus, at high temperatures, the increase of conductivity which contribute to the lose factor could cover up the extrinsic contribution of domain wall motions. For this reason, we have to compare the measured results from both low and high field strength at the same temperatures in order to see the contribution

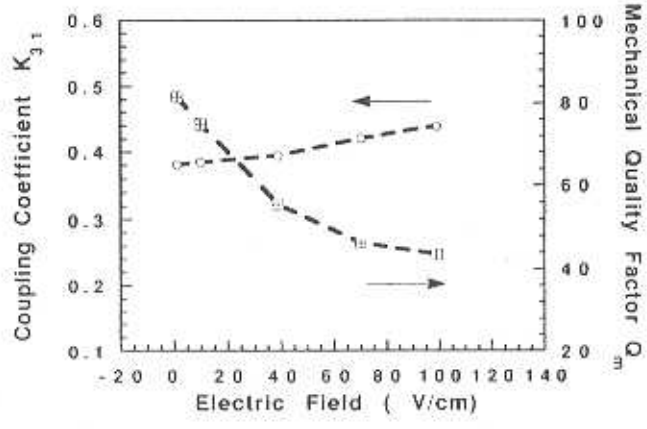

FIGURE 12 Variation of the electromechanical coupling factor k_{31} and the mechanical quality factor Q_m due to the increase of the applied a.c. electric field strength.

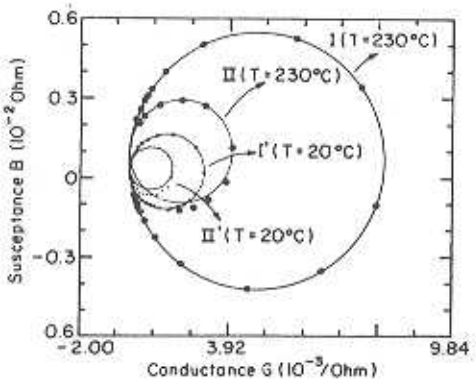

FIGURE 13 Susceptance (B) v.s. conductance (G) loops for a soft PZT ceramic at two different applied a.c. field strengths and two different temperatures.

TABLE II

Electromechanical coupling factors, piezoelectric coefficients and mechanical quality factors of PZT-5A ceramic at different temperatures and field levels

	T = 20 °C			T = 230 °C		
	k_{31}	Q_m	d_{31}	k_{31}	Q_m	d_{31}
E= 70 V/cm	0.418	47	-186	0.36	52.4	-218
E= 1 V/cm	0.387	80	-179	0.28	182	-195

of domain wall motions. Figure 13 presents the complex admittance circles of a PZT-5 ceramic resonator measured with two different applied field strengths at two different temperatures. The radii of these four circles are denoted by B_1, B_2, B_1', and B_2', respectively. Here B_1' (low drive level) and B_2' (high drive level) are for the room temperature measurements, B_1 (low drive level) and B_2 (high drive level) are for the measurements made at T = 230°C. It could be found that the ratio of (B_1/B_2) increases with temperature. The ratio of (B_1/B_2) is proportional to the nonlinear mechanical losses of the ceramic resonator in the vicinity of the resonance frequency, because the radii of these circles are proportional to the mechanical quality factor Q_m.[61] Table II lists the electromechanical coupling and piezoelectric coefficients as well as the mechanical quality factor for different temperatures and different drive levels. These results convincingly show that the increase of electromechanical coupling as the temperature increases arises from the increase of domain wall mobility.

V. SUMMARY

We have measured the dielectric and piezoelectric properties of PZT system in several compositions at both high and low field levels. The experimental results show that domain wall vibrations contribute significantly to the electromechanical nonlinearity in ferroelectric ceramics. The main results are summarized as follows:

1. A phenomenological model has been extended to evaluate the macroscopic nonlinear parameters associated with non-180° domain wall vibrations in ferroelectric ceramics. The theoretical description qualitatively agrees with some of the experimental results.
2. Dielectric and piezoelectric measurements have been carried out for PZT ceramic system at different field levels and temperatures, the results are compared with the theoretical model. It has been verified that the couplings between the acoustic vibrations and the movement of domain walls is an important factor in terms of extrinsic properties of ferroelectric ceramics. It is found that the nonlinear effects are extrinsic in nature and will easily occur at the resonant frequency because the coupling interaction between domain wall motions and the acoustic waves is maximum at the resonant frequency. The piezoelectric and dielectric coefficients and losses in the nonlinear regime are much larger than those in the linear regime. The threshold fields of the dielectric and piezoelectric coefficients are strongly affected by the bias field, temperature and compositions.
3. PZT ceramic with composition near the morphotropic phase boundary shows a pronounced maximum of the non-linear effect. The ratio of c/a axes is an important factor which affects the extrinsic properties in PZT ceramic system. Both shifts of f_m and f_n of the admittance at the high drive level due to the nonlinearity could be evaluated from non-180° domain wall motion. It has been suggested previously[31] that the nonlinear effects in the resonance frequency region originates from the collective resonance of domain walls. This opinion is questionable because the resonance frequency of ceramic samples depends on the sample size and is usually much lower than the domain wall resonance frequency. However, since the resonance frequency of domain walls is still a disputed topic, further investigation is required. We believe that the nonlinear effects contain both intrinsic and extrinsic contributions. In multidomain crystals, such as ferroelectric ceramics, the extrinsic contributions play the dominant role in generating these nonlinearities.

ACKNOWLEDGEMENTS

We thank Professor A. S. Bhalla for some stimulating discussions, Dr. D. Damjanovic for his assistance in the iterative method calculation and providing us with the computer program and Dr. U. Kumar for his assistance in preparing ceramic samples. This research was supported by the Office of Naval Research under grant No. N00014-89-J-1689.

REFERENCES

1. P. Gonnard, L. Eyraud, M. Troccaz and P. Eyraud, "Analysis of the Suitability of Piezoceramics for High Power Transducers," *Proc. IEEE. Ultrasonics Symposium*, 619–623 (1986).
2. Ralph S. Woollett and Charles L. Leblanc, "Ferroelectric Nonlinearities in Transducer Ceramics," *IEEE Transactions on Sonics and Ultrasonics*, **SU-20**(1), 24–31 (1973).
3. D. A. Berlincourt, D. R. Curran and H. Jaffe, "Piezoelectric and Piezomagnetic Materials and Their Function in Transducers," *Physical Acoustic*, **1**(A), Chapter 3, Ed. by W. P. Mason, Academic Press, NY (1964).
4. J. M. Huckabay, Hollis C. Boehem and Elmer L. Hixson, "Admittance Measurement Accuracies Required to Determine Nonlinear Behavior in Sonar Transducers," *IEEE Transactions on Sonics and Ultrasonics*, **SU-22**(2), 101–104 (1975).

5. K. Lubitz and W. Wersing, "Automatic Performance Testing of Piezoelectric Ceramics for Power Transducers," *Ferroelectrics*, **40**, 237–244 (1982).
6. K. Uchino, Kiroyasu Negishi and Terukiyo Hirose, "Drive Voltage Dependence of Electromechanical Resonance in PLZT Piezoelectric Ceramics," *J. of Appl. Phys.*, Vol. **28**, Supplement **28-2**, 47–49 (1989).
7. R. Lee and J. F. Vetelino, "Influence of an External Electric Field on the Electroacoustic Properties of PZT-4," *Proc. IEEE. Ultrasonics Symposium*, 741–745 (1987).
8. E. A. Kraut, T. C. Lim and B. R. Tittmann, "Application of Nonlinear Interactions in Ferroelectric Ceramics to Microwave Signal Progressing," *Ferroelectrics*, **3**, 247–255 (1972).
9. A. Oliver, "Acoustic Surface Waves," Springer, New York (1978).
10. R. E. Newnham, Q. C. Xu, S. Kumar and L. E. Cross, "Smart Ceramics," *Ferroelectrics*, **102**, 1–8, (1990).
11. A. F. Devonshire, "Theory of Barium Titanate—Part 1," *Phil. Mag.* **40**, 1040–1049 (1949).
12. M. J. Haun, E. Furman, S. J. Jang and L. E. Cross, "Thermodynamic Theory of the Lead Zirconate—Titanate Solid Solution System, Part I: Phenomenology," *Ferroelectrics*, **99**, 13–25 (1989).
13. G. Arlt, H. Dederichs and R. Herbiet, "90°-domain Wall Relaxation in Tetragonally Distorted Ferroelectric Ceramics," *Ferroelectrics*, **74**, 37–53 (1987).
14. G. Arlt and H. Dederichs, "Complex Elastic, Dielectric and Piezoelectric Constants by Domain Wall Damping in Ferroelectric Ceramics," *Ferroelectrics*, **29**, 47–50 (1980).
15. P. Gurk, "Contribution of Domain Wall Motion to the Permittivity of Rochelle Salt," *Phys. Stat. Sol.(a)*, **10**, 407–414 (1972).
16. V. A. Isupov, "Characteristics of Coexistence of Tetragonal and Rhombohedral Phases in Piezoelectric Ceramics Based on $PbTiO_3$ and $PbZrO_3$," *Sov. Phys. Solid State*, **18**(4), 529–534 (1976).
17. A. G. Luchaninov, A. V. Shil'Nikov, L. A. Shuvalov and I. JU. Shipkova, "The Domain Processes and Piezoeffects In Polycrystalline Ferroelectrics," *Ferroelectrics*, **98**, 123–126, (1989).
18. E. K. W. Goo, R. K. Mishra and G. Thomas, "Electron Microscopy Study of the Ferroelectric Domains and Domain Wall Structure in $PbZr_{0.52}Ti_{0.48}O_3$," *J. Appl. Phys.*, **52**(4), 2939–2943 (1981).
19. P. G. Lucuta, V. Teodoresu and F. Vasiliu, "SEM, SAED, and TEM Investigations of Domain Structure in PZT Ceramics at Morphotropic Phase Boundary," *Appl. Phys.*, **A37**, 237–242 (1985).
20. P. G. Lucuta, "Ferroelectric-Domain Structure in Piezoelectric Ceramics," *J. Am. Ceram. Soc.*, **72**(6), 933–937 (1989).
21. G. Arlt, "The Role of Domain Wall on the Dielectric, Elastic and Piezoelectric Properties of Ferroelectric Ceramics," *Ferroelectrics*, **76**, 451–458 (1987).
22. G. Arlt, "Microstructure and Domain Effects in Ferroelectric Ceramics," *Ferroelectrics*, **91**, 3–7 (1989).
23. R. Herbiet, U. Robels, H. Dederichs and G. Arlt, "Domain Wall and Volume Contributions to Materials Properties of PZT Ceramics," *Ferroelectrics*, **98**, 102–121 (1989).
24. E. I. Eknadiosiants, V. Z. Borodin, V. G. Smotrakov, V. V. Eremkin and A. N. Pinskaya, "Domain Structure of Rhombohedral $PbTi_xZr_{1-x}O_3$ Crystals," *Ferroelectrics*, **111**, 283–289 (1990).
25. L. Pardo, J. Mendiola, A. Gonzalez and J. De Frutos "Role of Domains on the Electromechanical Anisotropy of Ca-Modified $PbTiO_3$ Ceramics," *Ferroelectrics*, **94**, 189–194 (1989).
26. J. Von Cieminski, C. Kleint, H. Beige and R. Hoche, "Effects of Internal Mechanical Stress on the Electromechanical Properties of Ferroelectric Ceramics," *Ferroelectrics*, **109**, 95–100 (1990).
27. D. Berlincourt and H. A. Krueger, "Domain Processes in Lead Titanate Zirconate and Barium Titanate Ceramics," *J. of Appl. Phys.*, **30**, 1804–1810 (1959).
28. H. Beige and G. Schmidt, "Electromechanical Resonances for Investigating Linear and Nonlinear Properties of Dielectrics," *Ferroelectrics*, **41**, 39–49 (1982).
29. M. D. Bryant and R. F. Keltie, "A Characterization of the Linear and Non-linear Dynamic Performance of a Practical Piezoelectric Actuator, Part. 1: Measurements," *Sensors and Actuators*, **9**, 95–103 (1986).
30. M. D. Bryant and R. F. Keltie, "A Characterization of the Linear and Non-linear Dynamic Performance of a Practical Piezoelectric Actuator, Part. 2. Theory," *Sensors and Actuators*, **9**, 105–114 (1986).
31. A. F. Litvin, M. M. Pikalev, V. A. Doroshenko and V. Z. Borodin, "Electromechanical Nonlinearity of Polycrystalline Ferroelectrics Under Resonant Excitation," *Ferroelectrics*, **51**, 159–171 (1984).
32. H. J. Hagemann, "Loss Mechanisms and Domain Stabilization in Doped $BaTiO_3$," *J. Phys. C.*, **11**, 3333–3344 (1978).
33. Shaoping Li, Wenwu Cao and L. E. Cross, "The Extrinsic Nature of Nonlinear Behavior Observed in Lead Zirconate Titanate Ferroelectric Ceramics," *J. Appl. Phys.*, **69**, 7219–7224 (1991). Shaoping Li, "Extrinsic Contributions to the Response in Ferroelectric Ceramics," Ph.D. Thesis, The Pennsylvania State University (expected 1992).

34. A. S. Nowick and W. R. Heller, "Anelasticity and Stress-Induced Ordering of Point Defects in Crystals," *Adv. in Phys.*, **12**, 251–298 (1963).
35. A. S. Nowick and W. R. Heller, "Dielectric and Anelastic Relaxation of Crystals Containing Point Defects," *Adv. in Phys.*, **14**, 101–164 (1965).
36. R. E. Nettleton, "Effective Mass of 180° Domain Wall in Single Crystal Barium Titanate," *J. of Physical Society of Japan*, **22**(6), 1375–1386 (1967).
37. R. C. Miller and G. Weinreich, "Mechanism for the Sidewise Motion of 180° Domain Walls in Barium Titanate," *Phys. Rev.*, **117**, 117 (1960).
38. J. Fousek and B. Brezina, "Relaxation of 90°-Domain Walls of $BaTiO_3$ and Their Equation of Motion," *J. Phys. Soc. of Japan*, **19**(6), 830–838 (1964); and "Frequency Dependence of the Motion of 90° Domain Walls in Barium Titanate," *Bulletin of the Academy of Science of the USSR*, **28**, 624–628 (1964).
39. J. Fousek and B. Brezina, "The Movement of Single 90° Domain Walls of $BaTiO_3$ in an Alternating Electric Field," *Czech. J. Phys.*, **B10**, 511–528 (1960), and "The Motion of 90° Wedge Domains in $BaTiO_3$ in an Alternating Electric Field," *Czech. J. Phys.*, **B11**, 344–359 (1961).
40. G. Arlt and N. A. Pertsev, "Force Constant and Effective Mass of 90° Domain Walls in Ferroelectric Ceramics," *J. Appl. Phys.*, **70**(4), 2283–2289 (1991).
41. V. S. Postnikov, V. S. Pavlov, and S. K. Turkov, "Internal Friction in Ferroelectrics Due to Interaction of Domain Boundaries and Point Defects," *Phys. Chem. Solids*, **31**, 1785–1791 (1970).
42. V. S. Postnikov, V. S. Pavlov, and S. K. Turkov, "Internal Friction in $Pb_{0.95}Sr_{0.05}(Zr_{0.53}Ti_{0.47})O_3$ + 3% PbO Ferroelectric Ceramics," *Izv. Akad. Nauk.*, **31**, 1845–1850 (1967).
43. V. S. Postnikov, V. S. Pavlov, S. A. Gridnev, and S. K. Turkov, "Interaction Between 90° Domain Walls and Point Defects on the Crystal Lattice in Ferroelectric Ceramics," *Soviet Physics—Solid State*, **10**(6), 1267–1271 (1968).
44. Jan G. Smits, "Influence of Moving Domain Walls and Jumping Lattice Defects on Complex Material Coefficients of Piezoelectrics," *IEEE Transactions on Sonics and Ultrasonics*, **SU-23**(3), 168–174 (1976).
45. J. O. Gentner, P. Gerthsen, A. Schmidt, and R. E. Send, "Dielectric Losses in Ferroelectric Ceramics Produced by Domain Wall Motion," *J. Appl. Phys.*, **49**(8), 4485–4489 (1978).
46. A. H. Nayfeh, "Perturbation Methods," John Wiley & Sons Inc. (1973).
47. C. E. Land and W. D. Smith, *Appl. Phys. Lett.*, **23**, 57–60 (1973).
48. I. P. Kaminow, "An Introduction to Electric-optic Devices," Academic Press, New York (1974).
49. J. R. Maldonado and A. H. Meitzler, "Ferroelectric Domain Switching in Rhombohedral-Phase PLZT Ceramics," *Ferroelectrics*, **3**, 169–175 (1972).
50. C. J. Burfoot, and G. W. Taylor, "Polar Dielectrics and Their Applications," 304, The Macmillan Press Ltd. (1979).
51. R. E. Newnham, "Domains in Minerals," *Amer. Miner.*, **59**, 906–918 (1974).
52. G. Arlt, "Domain Contributions to Piezoelectricity in Ceramics," *IEEE, 1990 Ultrasonic Symposium*, 733–738 (1990).
53. Jan G. Smits, "Iterative Method for Accurate Determination of the Real and Imaginary Parts of the Materials Coefficients of Piezoelectric Ceramics," *IEEE Transactions on Sonic and Ultrasonics*, **SU-23**(6), 393–402 (1976).
54. Q. M. Zhang, W. Y. Pan and L. E. Cross, "Laser Interferometer for the Study of Piezoelectric and Electrostrictive Strains," *J. Appl. Phys.*, **68**(8), 2492–2496 (1988).
55. L. Benguigui, "Ferroelectric Losses in $BaTiO_3$ Produced by the 90° Domain Walls," *Ferroelectrics*, **7**, 315–317 (1974).
56. D. G. Sannikov, "Dispersion in Ferroelectrics," *Soviet Physics JETP*, **14**, 98–101 (1962).
57. P. Gerthsen, K. H. Hardtl, and N. A. Schmidt, "Correlation of Mechanical and Electrical Losses in Ferroelectric Ceramics," *J. Appl. Phys.*, **51**(2), 1131–1134 (1980).
58. Seiji Ikegami, and Ichiro Ueda, "Mechanism of Aging in Polycrystalline $BaTiO_3$," *J. of the Physical Society of Japan*, **22**(3), 725–734 (1967).
59. D. Berlincourt, B. Jaffe, H. Jaffe and H. H. A. Krueger, "Transducer Properties of Lead Titanate Zirconate," *IRE Trans. Ultrasonics Eng.*, 1–7 (1960).
60. J. G. Smits, "Eigenstates of Coupling Factors and Loss Factor of Piezoelectric Ceramics," Ph.D. Thesis Twente University of Technology, Netherlands (1978).
61. Takuro Ikeda, "Fundamentals of Piezoelectricity," Oxford University Press (1990).